Chapter 3

ELECTROCHEMICAL AMMONIA PRODUCTION BY A SURFACE-ATTACHED IRON COMPLEX

3.1 INTRODUCTION

The reduction of N_2 to NH_3 is an essential transformation for life and is performed on a massive scale both industrially and biologically.[1–3] The high stability of the N≡N triple bond necessitates a catalyst to achieve this transformation selectively.[4] Assembling systems for the conversion of solar energy to NH_3 requires the development of electrodes capable of selective reduction of N_2 to NH_3.[5–8] Inorganic complexes have attracted significant attention as homogeneous catalysts for N_2 reduction, although electrochemical N_2 reduction by molecular complexes remains challenging.[9] Immobilization of molecular catalysts on electrode surfaces presents further challenges; immobilization methods require harsh conditions with limited functional group compatibility and are often not general.[10] In principle, attachment of molecular catalysts onto conducting electrodes allows their thorough investigation by electrochemical methods, delivering a deeper understanding of the mechanisms and redox events involved in the catalytic process. Surface attachment may also provide further benefits, such as higher stability, decrease in potentially deleterious bimolecular pathways, and ability to operate in a broader range of solvents.[8, 11]

Attachment of a molecular N_2 reduction catalyst to an electrode would demonstrate the compatibility of surface immobilization strategies with conditions required to effect N_2 reduction, as well as allow further study of the immobilized species by electrochemical and spectroscopic methods. Non-covalent attachment between a pyrene-appended electrocatalyst and a graphitic surface has been applied successfully to the hydrogen evolution reaction (HER), the carbon dioxide reduction reaction (CO_2RR), and the oxygen evolution reaction (OER).[10] This attachment strategy requires modification and new synthetic methods, and often requires multiple pyrene groups to provide long-lived surface-bound species.[12, 13] Furthermore, it is unclear if this attachment strategy is compatible with the highly reducing potentials required for N_2 reduction. Herein we report the electrochemical production of ammonia by a P_3^BFe complex immobilized on a graphite electrode through three tethered pyrene groups.

3.2 RESULTS AND DISCUSSION

Recently, our group reported the electrocatalytic reduction of N_2 to NH_3 using a cocatalytic electron mediator. Controlled potential electrolysis (CPE) at -2.1 V vs $Fc^{+/0}$ with a glassy carbon plate electrode using $P_3^BFe^+$ as a precatalyst in the presence of $[Ph_2NH_2][OTf]$ acid and $[Cp^*{}_2Co][BAr^F{}_4]$ gave 5.5 equiv of NH_3 per Fe.[9c] This catalysis occurs slowly, consuming 100 equiv acid per Fe over the course of ca. 35 hours. To increase the rate of catalysis and limit unproductive bimolecular pathways, we sought to immobilize a P_3^BFe species on a carbon surface.

Scheme 3.1

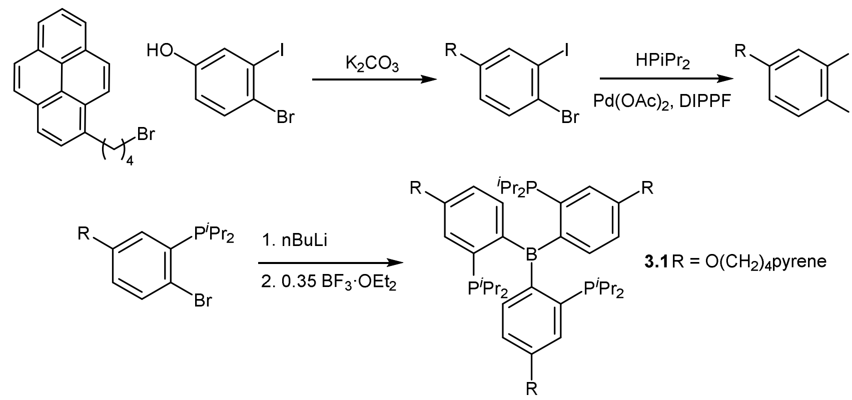

To immobilize P_3^BFe on a carbon surface, the ligand framework was modified to incorporate three pyrene groups through a butoxy linker (Scheme 3.1). Pyrene groups were attached to the ligand aryl backbone through alkylation of 3-bromo-2-iodophenol with 1-(4-bromobutyl)pyrene followed by cross-coupling with HP*i*Pr₂. Lithiation and reaction with $BF_3 \cdot OEt_2$ in toluene/Et_2O then afforded the desired $^{py}P_3^B$ ligand (**3.1**). Metalation with $FeBr_2$ and reduction with Na/Hg afforded $^{py}P_3^BFeBr$ (**3.2**) as a red solid. Reaction with methyllithium then gave $^{py}P_3^BFeMe$ (**3.3**), which was purified by extraction with benzene (Scheme 3.2).

Scheme 3.2

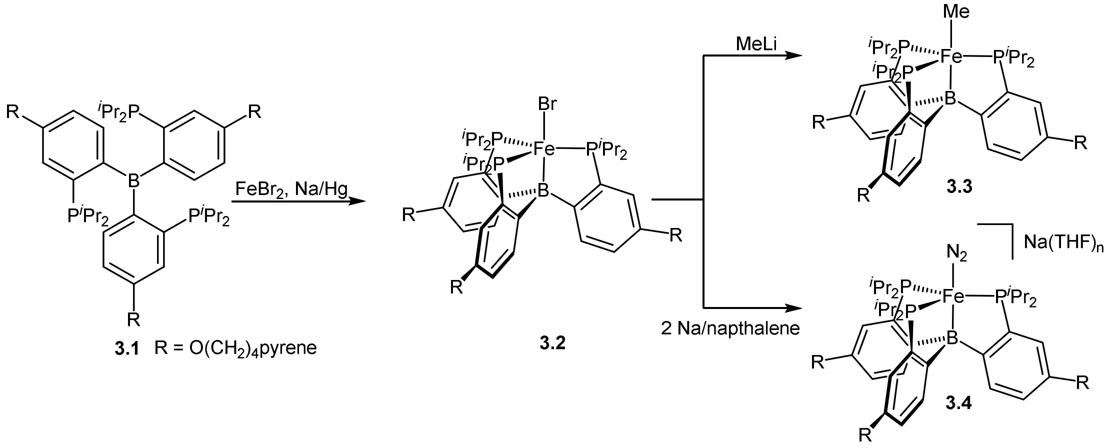

Reduction of **3.2** with 2 equiv of Na/naphthalene at -78 °C yields $[^{py}P_3^BFeN_2][Na(THF)_n]$ (**3.4**). The IR spectrum of **3.4** shows two intense N_2 stretching bands at 1930 cm^{-1} and 1880 cm^{-1}, which are attributable to the free anion $^{py}P_3{}^BFeN_2{}^-$ and tight ion pair $^{py}P_3{}^BFeN_2\cdots Na$, respectively.[14] Cyclic voltammetry of **3.4** on a glassy carbon electrode shows a reversible oxidation event at –2.2 V vs $Fc^{+/0}$ in 0.1 M $NaBar^F{}_4/Et_2O$, compared to $^-$2.1 V vs $Fc^{+/0}$ for the parent $P_3{}^BFeN_2{}^{0/-}$ couple.[9c]

We next investigated the N_2 fixation ability of $^{py}P_3{}^BFeMe$. We hypothesized that $^{py}P_3{}^BFeMe$ would serve as a suitable complex for surface attachment due to its high stability relative to $[^{py}P_3{}^BFeN_2][Na(THF)_n]$, and therefore sought to probe its chemical reactivity to determine if it could serve as a suitable precatalyst for N_2 reduction. Reaction of $^{py}P_3{}^BFeMe$ with 108 equiv $[Ph_2NH_2][OTf]$ acid and 54 equiv $Cp^*{}_2Co$ reductant at –78 ˚C in Et_2O gave 6.5 equiv NH_3 per Fe, demonstrating the viability of $^{py}P_3{}^BFeMe$ as a precatalyst for the reduction of N_2 to NH_3.

To study the electrochemistry and stability of $^{py}P_3{}^BFeMe$ immobilized on a surface, functionalized electrodes were prepared. The precatalyst was immobilized on the surface by soaking rectangular plates (10 mm x 15 mm x 1 mm) of basal plane highly ordered pyrolytic graphite (HOPG) electrodes in a 1 mM THF solution of $^{py}P_3{}^BFeMe$ for 16 hours, followed by rinsing with THF to remove any loosely bound species. The stability of $^{py}P_3{}^BFeMe$ to surface attachment was probed by analysis upon desorption by soaking in THF solution (Figure 3.1). UV-visible spectroscopy of **3.3** recovered from a functionalized electrode matched that of an authentic sample, demonstrating that **3.3** is appended to an electrode without decomposition. In total, 27 nmol cm^{-2} of **3** was recovered.

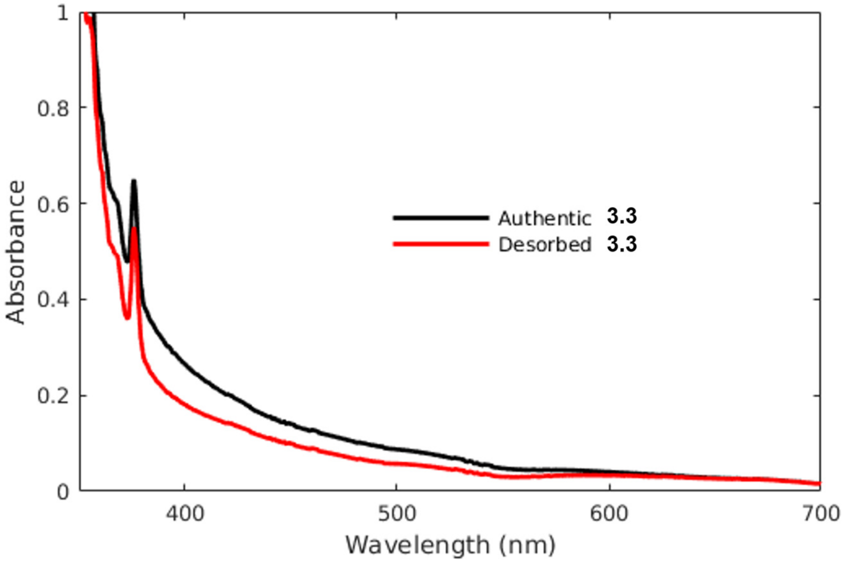

Figure 3.1: UV-vis spectra of authentic sample of **3.3** (black) and sample of **3.3** recovered from functionalized electrode (red).

Cyclic voltammetry of **3.3** immobilized on an HOPG electrode shows an irreversible reduction feature with an onset of –2.1 V vs $Fc^{+/0}$ (Figure 3.2). Upon addition of $[Ph_2NH_2][OTf]$ at –35 ˚C, current enhancement is observed with an onset of –1.8 V vs $Fc^{+/0}$, consistent with current enhancement previously observed with $P_3^BFe^+$ in the presence of acid.[9c]

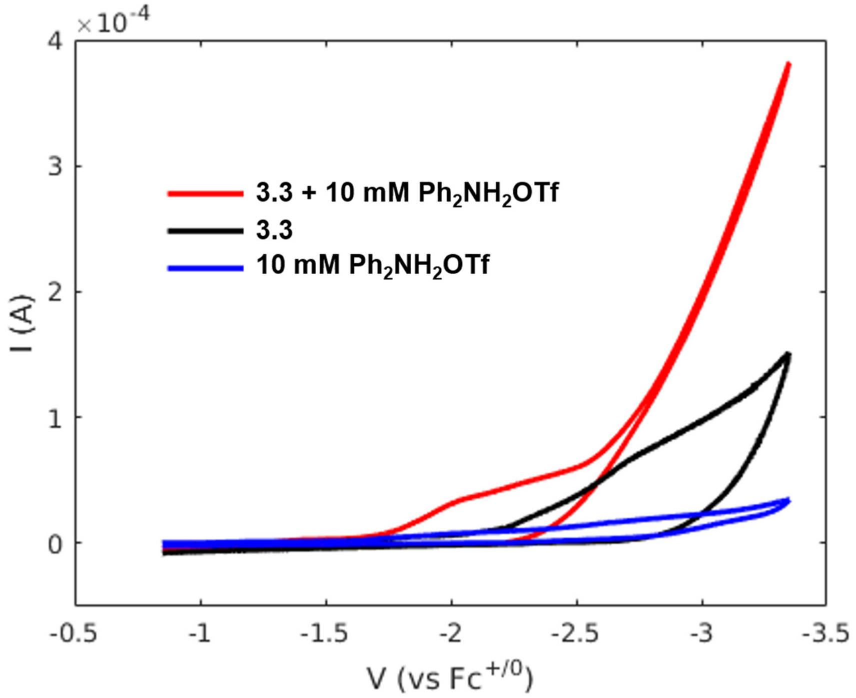

Figure 3.2: Cyclic voltammograms of unfunctionalized electrode in the presence of 10 mM [Ph_2NH_2][OTf] acid (blue trace), electrode functionalized with **3.3** in the absence of acid (black trace), and electrode functionalized with **3.3** in the presence of 10 mM [Ph_2NH_2][OTf] acid (red trace). All voltammograms are collected with a scan rate of 50 mV/s in 0.1 M $NaBAr^F_4$ solution in Et_2O at –35 ˚C and externally referenced to the $Fc^{+/0}$ couple.

To determine the product profile upon reduction, CPE experiments were conducted in the presence of 100 μmol [Ph_2NH_2][OTf] (Table 3.1). Over a 6 h period at –2.4 V vs $Fc^{+/0}$, 9.6 C net charge was passed, consistent with nearly full consumption of acid. 1.4 equiv NH_3 were produced per Fe, as determined by the indophenol method. Over the course of the 6 h electrolysis, the current remained above background but decreased at a rate of roughly 10% per hour, likely due to a combination of acid consumption and desorption of the catalyst from the electrode. XPS measurements on electrodes post-electrolysis shows decreased signals for Fe and P after 6 hours, consistent with partial desorption of $^{py}P_3{}^{B}Fe$ (Figure 3.3).

Table 3.1: Yields of NH_3 from CPE experiments with $^{py}P_3{}^{B}FeMe$-functionalized electrodes.

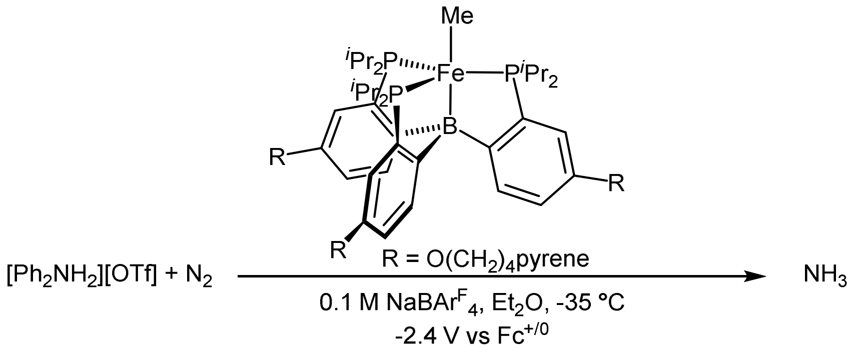

entry	hours	charge passed (C)	equiv (per Fe)	Faradaic Efficiency (H_2)
1	6.0	9.6(3)[a]	1.4(1)	89(2)
2[b]	6.0	0.7	<0.2[c]	92
3[d]	6.0	2.7	<0.2[c]	90

[a] Average of two runs [b] Bare HOPG electrode. [c] Relative to Fe loading in entry 1. [d] HOPG electrode functionalized with ligand **3.1**.

To demonstrate that $^{py}P_3{}^{B}FeMe$ is required for NH_3 production, a CPE experiment was conducted employing a non-functionalized electrode. This electrolysis gave <0.2 equiv NH_3 over 6 h, with a net charge of 0.7 C passed. To then demonstrate that Fe is required for NH_3 production, electrodes were functionalized with $^{py}P_3{}^{B}$ and employed in CPE experiments. Over 6 h, <0.2 equiv NH_3 was produced, with a net charge of 2.7 C passed. This increased current relative to a bare electrode may be due to protonation of the surface-bound ${}^{py}P_3{}^{B}$, which would increase the acid concentration at the electrode and facilitate proton reduction.

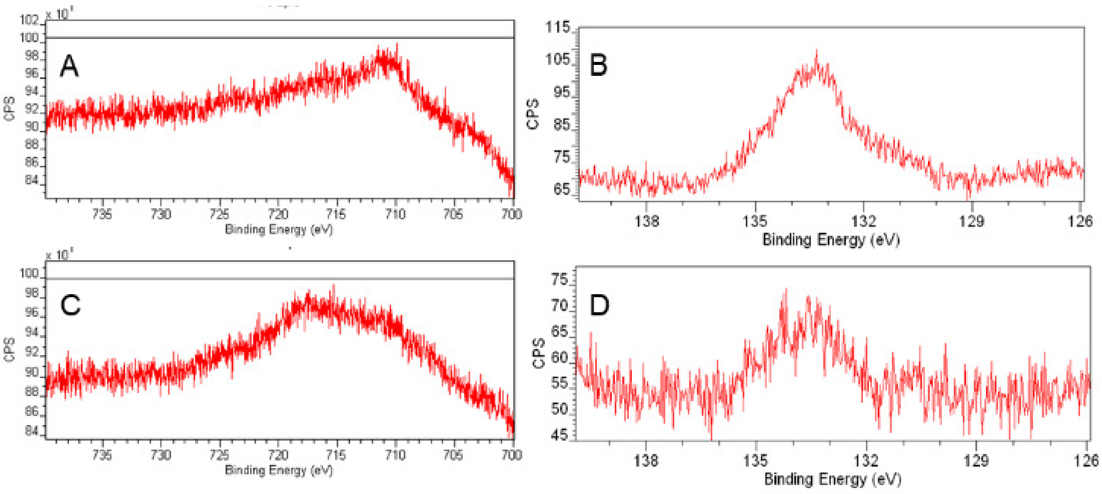

Figure 3.3: XPS spectra of an HOPG electrode with immobilized **3.3** (A) in the Fe 2p region pre-electrolysis, (B) in the P 2p region pre-electrolysis, (C) in the Fe 2p region post-electrolysis, and (D) in the P 2p region post-electrolysis.

3.3 CONCLUSION

In summary, we have demonstrated electrochemical production of NH_3 from a ${}^{py}P_3{}^{B}FeMe$ species immobilized on a graphite surface. To our knowledge, this is the first report of surface attachment of a molecular N_2 reduction catalyst. The functionalized electrode displays reasonable stability over the course of 6 h despite the highly reducing potentials required for N_2 reduction. This stability demonstrates that electrode surface attachment strategies are compatible with the highly reducing potentials required for electrochemical N_2 reduction, and will aid in the optimization and study of N_2 reduction by immobilized catalysts.

3.4 REFERENCES

(1) Smil, V. Enriching the Earth; MIT Press: Cambridge, Mass, 2001.

(2) Galloway, J. N.; Dentener, F. J.; Capone, D. G.; Boyer, E. W.; Howarth, R. W.; Seitzinger, S. P.; Asner, G. P.; Cleveland, C. C.; Green, P. A.; Holland, E. A.; et al. Nitrogen Cycles: Past, Present, and Future. *Biogeochemistry* **2004**, *70 (2)*, 153–226.

(3) Fowler, David; Coyle, Mhairi; Skiba, Ute; Sutton, Mark A.; Cape, J. Neil; Reis, Stefan; Sheppard, Lucy J.; Jenkins, Alan; Grizzetti, Bruna; Galloway, James N.; et al. The Global Nitrogen Cycle in the Twenty-First Century. *Philos. Trans. R. Soc. B: Biol. Sci.* **2013**, *368 (1621)*, 20130164.

(4) Ham, C. J. M. van der; Koper, M. T. M.; Hetterscheid, D. G. H. Challenges in Reduction of Dinitrogen by Proton and Electron Transfer. *Chem. Soc. Rev.* **2014**, *43 (15)*, 5183–5191.

(5) Shipman, M. A.; Symes, M. D. Recent Progress towards the Electrosynthesis of Ammonia from Sustainable Resources. *Catal. Today* **2017**, *286*, 57–68.

(6) Rosca, V.; Duca, M.; de Groot, M. T.; Koper, M. T. M. Nitrogen Cycle Electrocatalysis. *Chem. Rev.* **2009**, *109 (6)*, 2209–2244.

(7) Kyriakou, V.; Garagounis, I.; Vasileiou, E.; Vourros, A.; Stoukides, M. Progress in the Electrochemical Synthesis of Ammonia. *Catal. Today* **2017**, *286*, 2–13.

(8) Dalle, K. E.; Warnan, J.; Leung, J. J.; Reuillard, B.; Karmel, I. S.; Reisner, E. Electro- and Solar-Driven Fuel Synthesis with First Row Transition Metal Complexes. *Chem. Rev.* **2019**, *119 (4)*, 2752–2875.

(9) (a) Roux, Y.; Duboc, C.; Gennari, M. Molecular Catalysts for N_2 Reduction: State of the Art, Mechanism, and Challenges. *ChemPhysChem* **2017**, *18 (19)*, 2606–

2617. (b) Pickett, C. J.; Talarmin, J. Electrosynthesis of Ammonia. *Nature* **1985**, *317 (6038)*, 652. (c) Chalkley, M. J.; Del Castillo, T. J.; Matson, B. D.; Peters, J. C. Fe-Mediated Nitrogen Fixation with a Metallocene Mediator: Exploring pKa Effects and Demonstrating Electrocatalysis. *J. Am. Chem. Soc.* **2018**, *140 (19)*, 6122–6129. (d) Sherbow, T. J.; Thompson, E. J.; Arnold, A.; Sayler, R. I.; Britt, R. D.; Berben, L. A. Electrochemical Reduction of N_2 to NH_3 at Low Potential by a Molecular Aluminum Complex. *Chem. – Eur. J.* **2019**, *25 (2)*, 454–458. (e) Lindley, B. M.; van Alten, R. S.; Finger, M.; Schendzielorz, F.; Würtele, C.; Miller, A. J. M.; Siewert, I.; Schneider, S. Mechanism of Chemical and Electrochemical N_2 Splitting by a Rhenium Pincer Complex. *J. Am. Chem. Soc.* **2018**, *140 (25)*, 7922–7935. (f) Becker, J. Y.; Avraham (Tsarfaty), S.; Posin, B. Nitrogen Fixation: Part I. Electrochemical Reduction of Titanium Compounds in the Presence of Catechol and N_2 in MeOH or THF. *J. Electroanal. Chem. Interfacial Electrochem.* **1987**, *230 (1)*, 143–153. (g) Becker, J. Y.; Posin, B. Nitrogen Fixation: Part II. Nitrogen Reduction by Electrochemically Generated Vanadium(II) Promoted by Various Organic Ligands in Basic Methanol. *J. Electroanal. Chem. Interfacial Electrochem.* **1988**, *250 (2)*, 385–397.

(10) (a) Collman J. P.; Denisevich, P.; Konai, Y.; Marrocco, M.; Koval, C.; Anson, F. C. Electrode Catalysis of the Four-Electron Reduction of Oxygen to Water by Dicobalt Face-to-Face Porphyrins. *J. Am. Chem. Soc.* **1980**, *102 (19)*, 6027–6036. (b) Yao, S. A.; Ruther, R. E.; Zhang, L.; Franking, R. A.; Hamers, R. J.; Berry, J. F. Covalent Attachment of Catalyst Molecules to Conductive Diamond: CO_2 Reduction Using "Smart" Electrodes. *J. Am. Chem. Soc.* **2012**, *134 (38)*, 15632–

15635. (c) Axet, M. R.; Dechy-Cabaret, O.; Durand, J.; Gouygou, M.; Serp, P. Coordination Chemistry on Carbon Surfaces. *Coord. Chem. Rev.* **2016**, *308*, 236-345.

(11) Bullock, R. M.; Das, A. K.; Appel, A. M. Surface Immobilization of Molecular Electrocatalysts for Energy Conversion. *Chem. – Eur. J.* **2017**, *23 (32)*, 7626–7641.

(12) Mann, J. A.; Rodríguez-López, J.; Abruña, H. D.; Dichtel, W. R. Multivalent Binding Motifs for the Noncovalent Functionalization of Graphene. *J. Am. Chem. Soc.* **2011**, *133 (44)*, 17614–17617.

(13) Kohmoto, M.; Ozawa, H.; Yang, L.; Hagio, T.; Matsunaga, M.; Haga, M. Controlling the Adsorption of Ruthenium Complexes on Carbon Surfaces through Noncovalent Bonding with Pyrene Anchors: An Electrochemical Study. *Langmuir* **2016**, *32 (17)*, 4141–4152.

(14) Moret, M.-E.; Peters, J. C. Terminal Iron Dinitrogen and Iron Imide Complexes Supported by a Tris(Phosphino)Borane Ligand. *Angew. Chem. Int. Ed.* **2011**, *50 (9)*, 2063–2067.